Numerical Simulation of PCB-Coil-Layouts for Inductive Energy Transfer Systems

David Maier[*], Normen Lucht, Alexander Enssle, Anna Lusiewicz, Julian Fischer, Urs Pecha, Prof. Dr.-Ing. Nejila Parspour
University of Stuttgart, Institute of Electrical Energy Conversion, Pfaffenwaldring 47, 70569 Stuttgart, Germany *david.maier@iew.uni-stuttgart.de

Abstract: This paper presents the two dimensional (2D) Finite Element Method (FEM) COMSOL model of a PCB-Coil layout. The model comprises different coil layouts for a comparison. The scientific goal of the simulation is to find an optimized arrangement considering a high quality factor of the coil. The case of application for the simulated coils are inductive contactless energy transfer systems with a low magnetic coupling.

Keywords: Contactless energy transfer, wireless power transfer, AC/DC Module, PCB coil.

1. Introduction

Designing different coil arrangements for contactless energy transfer systems, further referred to by the acronym CET, became more and more advantageous and affordable with the use of FEM simulation in the last years. Beside numerical simulation, the magnetic parameters of the coil system are usually calculated with empiric findings or analytical calculations. These methods are easy to handle for systems with basic coil arrangements. With arrangements getting more complex, through either magnetic shielding, flux guidance or special coil geometries, the accuracy is getting worse. In addition to the aforementioned, the calculation of losses in the winding system is difficult to describe analytically and it profits from the increasing speed of the FEM simulation. The simulated coil system of this contribution uses a circular coil geometry without a flux guidance or shielding. To work out the optimized geometry for a high quality factor the model calculates direct- and alternating current losses like eddy currents. Compared to other simulations where only a part of the system has to be modeled, for example a three phase transverse flux machine [1], it is recommended to simulate the overall coil arrangement, because of a lack of repeatability. This significantly increases the computation time for 3D models. Furthermore, multiple simulations are performed to compare different geometries. Both the long computation time and the optimization process result in the choice to simulate the geometry in a 2D FEM COMSOL model, which is presented in this article.

2. Contactless energy transfer systems

In recent years, contactless inductive energy transfer systems have become more and more popular. Inductive CET systems are described principally in the same way as the well known transformer $(k \approx 1)$. A major difference is the low magnetic coupling between the primary side and secondary side coil, which is usually smaller than $k = 0.5$. For an efficient energy transfer the systems operating frequency is in the range of 20 kHz to several MHz [2]. Based on the weak coupling a CET system needs a reactive power compensation. Figure 1 shows the typical setup of an inductive CET system.
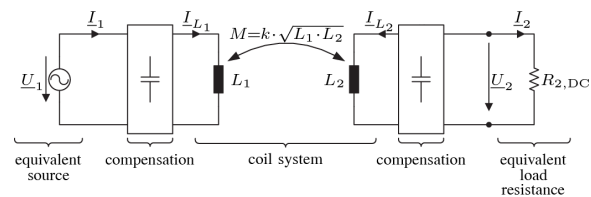
Figure 1. Overview of an inductive CET system with reactive power compensation and coil system [3].

The type of the reactive power compensation arrangement significantly affects the system behavior. With a primary and secondary side compensation with one capacitor, there are four possibilities to arrange the compensation, which is either in series or in parallel to the single coils. The respective system behavior of all four compensation topologies is described in detail in [4]. For example with the arrangement, it is possible to create either a constant current source or a constant voltage source on the secondary side. In addition primary side serial compensated systems are compared to parallel compensated systems not safe for idle operation, a short circuit or a removal of the secondary side [4]. In Figure 1 the rectifier and the inverter are neglected and represented by an equivalent source and load. To operate the system, a resonant frequency is set with the inverter. CET systems with four energy storages have up to three resonant frequencies depending on the value of the load resistance. Considering an efficient system it is advisable to select a resonant frequency, which is, with respect to the system bounda-

ries of inverter and rectifier, as high as the quality factor Q of the coil arrangement is increased with the higher frequency [5]. In virtue of the frequency, a high-frequency litz wire is used for technically practical coil systems. Whereas using a PCB coil with a layer thickness of 70 µm and a width of 2 mm on average, the influence of skin and proximity effect, due to the missing litz wire, is simulated with multiple single coils in the COMSOL model. In general, with a transferred constant power, the losses in the CET system are smaller with a higher frequency. This relationship is shown by three equations.

$$P = I_1^2 \cdot k \cdot \omega \cdot L_1 \ (1) \qquad\qquad P_V = R \cdot I^2 \ (2)$$

$$\delta \sim \sqrt{\frac{1}{\omega}} \ (3)$$

Equation 1 describes the transferred power of a both side serial compensated system, depending on input current I_1, coupling factor k, design frequency ω and the primary side inductance L_1 [4]. By neglecting the influence of parasitic capacitance, the primary inductance and the coupling factor are constant. Multiplying the resonant frequency ω by four, the resulting input current I_1' for the same transferred power $P = P'$ is gained with

$$I_1^2 \cdot k \cdot \omega \cdot L_1 = I_1'^2 \cdot k \cdot 4 \cdot \omega \cdot L_1$$

to

$$I_1' = \frac{I_1}{2} \ (4).$$

Further, the skin depth, calculated with proportionality 3, is reduced to a half. As long as the skin depth does not influence the current density inside the coil, the ohmic loss in Equation 3 is reduced with the higher frequency. As a result, the ratio between ohmic losses and the transferred power is getting smaller and this outcomes in a better efficiency as well as a higher quality factor.

In the COMSOL model the simulated PCB layer thickness is 70 µm at an average width of 2 mm. It is a scientific goal to evaluate the quality factor in an operating frequency range between 500 kHz and 1.5 MHz. Another goal is to evaluate different geometries. The used geometries are described in the following chapter.

3. Geometry and Materials

The PCB coil is designed as a double layer circular coil with a constant inner- and outer diameter. In a first step the geometry is modeled in 3D by the use of computer aided design methods. The result of a first coil arrangement is shown in Figure 2.
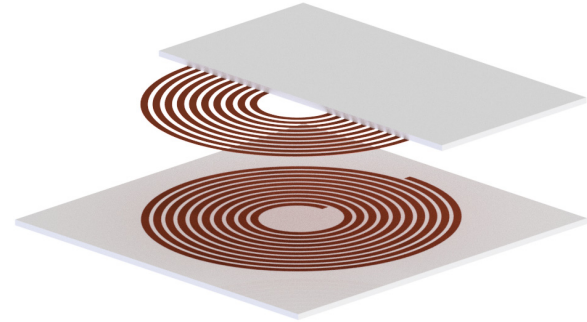
Figure 2. 3D model of the coil system with 10 copper windings and FR4 PCB board. For improved visibility, only one copper layer of the coil is shown.

The presented Figure 2 is created with Autodesk Inventor 2017. Using the LiveLink™ it is possible to import the complex geometry to the COMSOL 5.3 model as it is shown in [1]. Unfortunately, with the spiral geometry only 3D simulations are possible. To reduce the computation time for the optimization process the model is recreated as a 2D model in COMSOL. The following Figure 4 shows two different versions of the PCB coil.
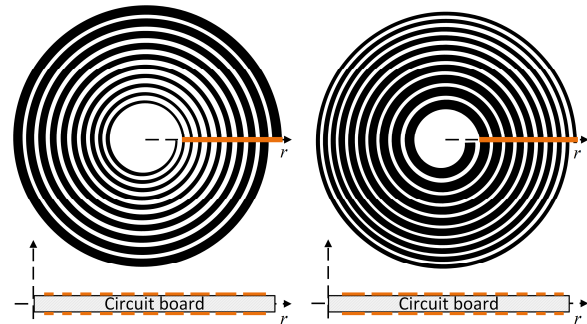
Figure 3. Geometry of printed circuit board; different coil arrangements; colored cut plane is used for approximate 2D simulation.

In the presented simulation multiple geometries between the left-sided and the ride-sided coil in Figure 3 are compared. The cut surface for the 2D model is derived out of the spiral coil at the position marked with an orange line. The resulting mapping of the COMSOL 2D geometry is presentend below each coil. According to the orange cut line, the value of the inner diameter is 20 mm and the outer diameter amounts to 80 mm. The simulations in this article are using a gap between each single winding with constant value of $a = 1$ mm and the winding number is set to $N = 10$. For the future optimization process these values are modified. The approch to parameterize the

model is to calulate the width of a single coil p for a coil with N turns with

$$\sum_{p=1}^{N} w(p) = r_o - r_i - (N-1) \cdot a \quad (5).$$

In this equation the width of a single coil is defined by w and the outer as well as the inner radius are defined by r_o and r_i. To parameterize the growth rate of the single coils, a ratio between the inner and outer winding is defined additionally.

The created 2D geometry in the COMSOL model has multiple air regions. Figure 4 shows the geometry with three defined air regions.
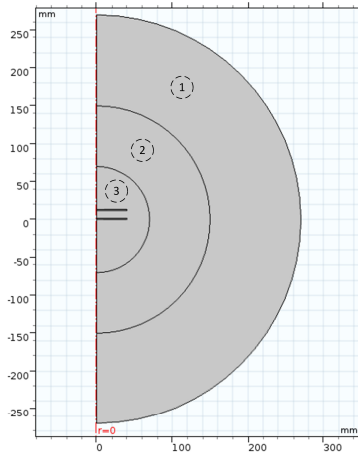
Figure 4. Geometry with three different air regions (1, 2 and 3) used to get a finer meshing. In the center primary- and secondary side 1.55 mm PCB with a 70 µm copper layer thickness.

In the center, two PCB coils for the primary and secondary side of the CET system are modeled as shown in Figure 3. The used materials for the regions are listed in Table 1.

Table 1: Material data

| Region	Material	Value
Airspace 1,2 and 3	Air	$\sigma = 0\,\mathrm{S \cdot m^{-1}}$
Coil winding	Copper	$\varepsilon_r = 1, \mu_r = 1$
Circuit board	FR4	$\varepsilon_r = 4.5$

4. Physics and solver

The model is solved with COMSOL's Magnetic and Electric Fields physics. To calculate magnetic parameters of a coil arrangement the Magnetic Field physics is sufficient. However, based on the PCB, with small distances and high frequency, the physics in this simulation is expanded to the calculation of the electric field. With this choice, the influence of parasitic capacitances is also simulated.

For the study a Frequency Domain is selected. The equations used in the simulation process are

$$\nabla \times H = J$$
$$B = \nabla \times A$$
$$E = -\nabla\, V_m - j\omega A \quad (6)$$
$$\nabla \cdot J = 0$$

for the magnetic and electric field. The simulation frequency of the Frequncy Domain study is set to 500 kHz and all results in this paper are computed with this frequency.

Owing to the low thickness of the PCB copper layer, the meshing process in this model is considered in detail. In Figure 5 a single copper winding is represented magnified.
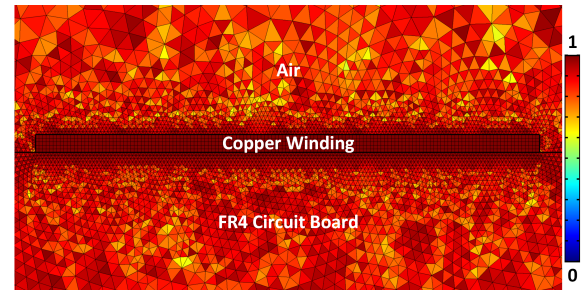
Figure 5. Mesh structure and quality of a single coil winding (approx. 70 µm in height and 2mm in length); quadrilateral and triangular mesh elements; legend from low (0) to high (1) quality.

To simulate the current density in the 70 µm copper layer a user-controlled mesh is selected and each region is defined itself. For the elements in the copper winding a quadrilateral mesh with an element size of 14 µm is selected. The mesh is getting coarser from extremely fine in the PCB up to normal in the outer air region. In 2D simulation no further settings are done. For the 3D simulation more meshing parameters like the maximum grow rate are tuned. Because of the small regions, the 3D simulation is very time consuming compared to the benefit. It is done in a second step with the optimized geometry and LiveLink™ for the Inventor CAD model, which is not part of this paper. An overview of the mesh data statistics is shown in Table 2.

Table 2: Mesh data

Properties	Approx. values
Number of elements	420000
Triangular	392000
Quadrilateral	28600
Mesh vertices	225000
Edge elements	14000
Vertex elements	180
Average element quality	0.8869
Minimum element quality	0.5269
Mesh area	114200mm²

For the computation of the Frequency Domain study, the direct MUMPS solver is used. In the model no further adjustment is done to optimize the solver. With the user-defined mesh a total of approximately 350.000 degrees of freedom are solved for the following results.

5. Results

On the one hand, the aim of several coil geometry simulations is to detect the amount and influence of eddy currents in the PCB windings and on the other hand, to identify the geometries with a high quality factor. In the post processing the 2D simulation is presented in 3D by the use of the Revolution 2D feature. In the resulting plot the magnetic flux density as well as the pattern of the magnetic field are shown in Figure 6.
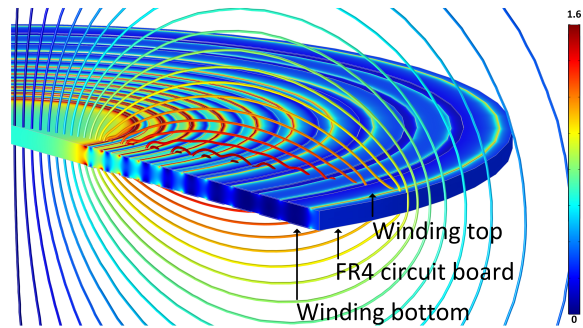
Figure 6. Primary coil with ten windings on each layer; absolute magnetic flux density in mT and pattern of magnetic field lines

For the rendering of Figure 6 the data set of the study solution was copied. In the first solution, all air regions are disabled in the selection feature, while in the second one all regions are present. For both solutions, a revolution is done. The shown surface flux density plot refers to the first data set with a revolution angle of 225 degrees. No air regions are visible in the surface plot. To display the magnetic field pattern the second data set is used. With a cut plane or a parametric surface it is possible to map the contour lines. The cut plane refers to the data set of the second revolution with all air regions selected.

The single coils on the top are connected with the coil group feature in series and the bottom coils are connected parallel to the top ones. In the simulation a current of 1 A excites each coil layer. For low eddy currents in the windings it is advisable to use many PCB layers, as long as every layer is at the same position in r-direction the amount of eddy currents is reduced in the layers below. Figure 6 represents this fact with the surface plot of the magnetic flux density. As it is seen underneath the single coil windings, there is

almost no magnetic field in this area, which would influence further copper winding layers.

In addition, another surface plot visualizes the influence of the skin depth. Based on equation

$$\frac{\mathrm{d}J_{\mathrm{phi}}}{\mathrm{d}r} \quad (7) \qquad \text{and} \qquad \frac{\mathrm{d}J_{\mathrm{phi}}}{\mathrm{d}z} \quad (8)$$

the current densities derivation is plotted on the surface by COMSOL with the commands

$$\text{d(mef.Jphi,r)} \qquad \text{and} \qquad \text{d(mef.Jphi,z)}$$

that are inserted in the surface plot expression field. Considering the resulting surface plot, it is obvious that the derivation in r-direction differs much more from the desired value of zero than the derivation in z-direction. This implies that the effect of skin depth is only influenced by the width of a single coil winding. The optimal solution without any effects of skin depth is a homogenous current density over the single coil windings with a derivation of zero. On this account, the following current density plot over the radius of the coil system is shown in Figure 7.
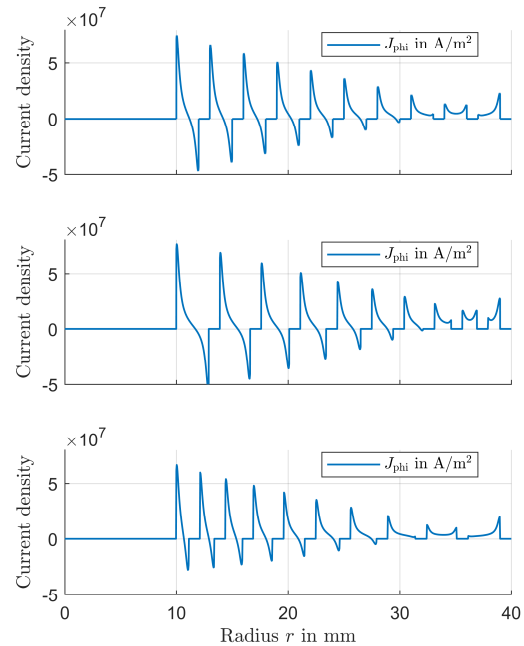

Figure 7. Current density measured in the center (35μm) of the top winding for three different coil arrangements

The current density J_{phi} is plotted for three different coil geometries. Relating to Figure 3 the bottom diagram represents the left geometry and the middle diagram the right geometry of Figure 3. The top picture of Figure 7 corresponds to an equal width of each

single coil winding. The three different plots are the result of a parametric sweep. J_{phi} is plotted by the use of a Cut Line 2D in the center (35µm) of the top coil layer. This line plot is sufficient because the derivation done with equation 8 showed a homogenous distribution in z-direction.

As it is seen, the single geometries have a different current density distribution over the radius. To interpret the current density the magnetic flux density is plotted over the radius in Figure 8.
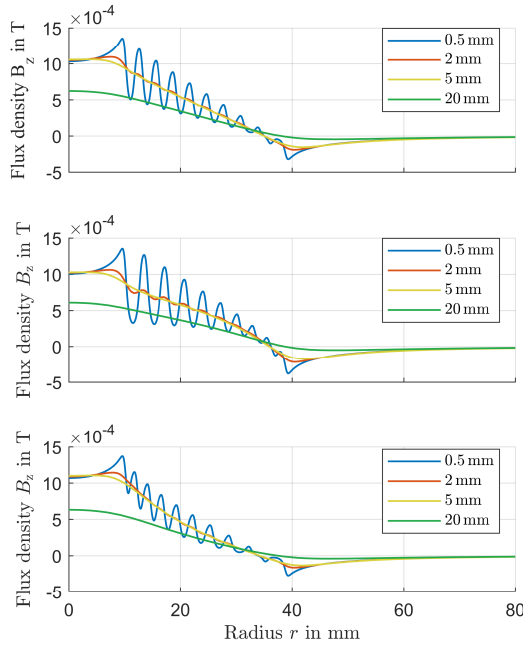
Figure 8. Magnetic flux density depending on the distance measured from the PCB's top etch layer for three different coil arrangements, see Figure 7

The single magnetic flux plots correspond to the same geometries like in Figure 7. It is visible that the coil geometry with the small inner and wide outer winding, plotted on the bottom of Figure 7 and Figure 8, has the lowest variation in the magnetic flux density as well as in the current density. This indicates that this geometry has the highest quality factor. With a global evaluation, the inductance as well as the losses of the winding are calculated. Solving for the quality factor leads to the best solution for this geometry. Nonetheless, the geometry with small inner windings has a lower inductance than the geometry with wide outer windings due to the smaller stretched area. Additionally the direct current losses are smaller with more copper surface, whereas the alternating current losses are bigger due to eddy currents in the copper surface.

The best geometry has a wide surface in the outer windings and a small surface in the inner windings, which reduces the direct current losses. In the center, the magnetic field is focused and eddy currents are induced. Due to the small surface, the amount of eddy currents is smaller than in the other case as it is shown in Figure 7. To evaluate the best geometry the gap between each winding and the number of turns should be taken into account. To automate the complex process COMSOLs optimization module is the best choice to find a solution.

6. Conclusions

This paper outlines the 2D simulation of a PCB coil for CET systems. It is shown that an optimization of the geometry increases the quality factor of a PCB coil. Besides changing the width of single windings, it is advisable to use the optimization toolbox of COM-SOL to modify more parameters of the system like winding numbers and the distance between the single windings. In a last step the optimized geometry of the 2D simulation should be imported to the 3D simulation and additionally the results should be compared with a manufactured PCB coil.

References

[1] S. Müller et al., "3D-FEM Simulation of a Transverse Flux Machine Respecting Nonlinear and Anisotropic Materials," in Comsol Conference 2016, COMSOL, Ed., 2016, pp. 1–6.

[2] M. Kazmierkowski and A. Moradewicz, "Unplugged But Connected: Review of Contactless Energy Transfer Systems," *EEE Ind. Electron. Mag.*, vol. 6, no. 4, pp. 47–55, 2012.

[3] M. Maier, D. Maier, M. Zimmer, and N. Parspour, "A novel self oscillating power electronics for contactless energy transfer and frequency shift keying modulation," in *2016 International Symposium on Power Electronics, Electrical Drives, Automation and Motion (SPEEDAM): 22-24 June 2016*, Piscataway, NJ: IEEE, 2016, pp. 67–72.

[4] D. Maier, J. Heinrich, M. Zimmer, M. Maier, and N. Parspour, "Contribution to the system design of contactless energy transfer systems," in *2016 IEEE International Power Electronics and Motion Control Conference (PEMC)*: IEEE, 2016, pp. 1008–1013.

[5] E. Waffenschmidt, "Wireless power for mobile devices," in 2011 IEEE 33rd International Telecommunications Energy Conference (INTELEC): IEEE, 2011, pp. 1–9.